PERGAMON

International Journal of Solids and Structures 40 (2003) 2121–2145

INTERNATIONAL JOURNAL OF SOLIDS and STRUCTURES

www.elsevier.com/locate/ijsolstr

Smoothing elastoplastic stress–strain curves obtained by a critical modification of conventional models

Chein-Shan Liu *

Department of Mechanical and Marine Engineering, National Taiwan Ocean University, Keelung 202-24, Taiwan, ROC

Received 30 April 2002; received in revised form 3 December 2002

Abstract

We first modify conventional one-dimensional perfectly elastoplastic constitutive model into a smooth one by shortening the switch-on time (or switch-on strain or switch-on stress) through a smooth factor ρ. This modification can be realized by assigning a piecewise constant yield stress $\sigma_y^m = [\sigma_y^0 + (\rho - 1)\sigma_{off}\mathrm{sgn}(\dot{\varepsilon})]/\rho$, whose ρ is proved to be in the range of $1 < \rho \leqslant 2$. When $\rho = 1$ we recover to the original model. By employing the same strategy to one-dimensional kinematic hardening model as well as to one-dimensional mixed-hardening model, we found that the newly modified models, besides provide a more smooth transition from elasticity to plasticity, are able to describe strain hardening effect, the Bauschinger effect, cyclic hardening effect, strain ratcheting behavior and even more complicated cyclic behavior. Then, we extend the same idea to modify a multi-dimensional mixed-hardening model. Instead of the conventional zero-measure yield surface, the new model allows plasticity to happen in some non-zero-measure yield volume in stress space, which is the main reason to cause smooth elastoplastic stress–strain behavior; moreover, the original yield surface has to be viewed mathematically as a limiting surface of the new model. Because the new model shares the same governing equations as the original model has, it is thermodynamically consistent as the original model is. From computational aspect, since stress points are no longer confined on the yield surface, the new model is more easily to numerically implement than the original model, and the conventional numerical design to match the consistency condition, e.g. the radial return method, is now no more needed for the new model.

Keywords: Elastoplasticity; Smooth factor; Bauschinger effect; Cyclic hardening; Strain ratcheting; Limiting surface

1. Introduction

Drucker (1988) has classified elastoplastic constitutive models into two types: conventional and unconventional. The conventional model is based on the assumption that the interior of yield surface is an elastic domain, wherein plastic deformation is not permitted no matter what stress changes occur. Conversely, the unconventional model under some conditions may allow plasticity to happen inside the yield surface. In order to differentiate these two situations Hashiguchi (1989) called the plastic state in which a

* Tel.: +886-2-2462-2192x3252; fax: +886-2-2462-0836.
E-mail address: csliu@mail.ntou.edu.tw (C.-S. Liu).

0020-7683/03/$ - see front matter © 2002 Elsevier Science Ltd. All rights reserved.
doi:10.1016/S0020-7683(03)00025-8

stress point lies on the conventional yield surface a "normal-yield state" and the plastic state within the yield surface a "subyield state".

The most frequently used conventional model is perfectly elastoplastic system (see, e.g., Liu, 2000) which allows plastic slip taking place at a constant value of applied stress and then leads to the tensile stress–strain curve being a horizontal line follows an inclined line. This is of course a very crude approximation to the elastoplastic stress–strain behavior of most metals. To enhance the simulation of experimentally observed hardening behavior in many metals strain-hardening was then proposed, which asserts that the yield surface expands with the amount of plastic flow. An alternative simple phenomenological mechanism, kinematic hardening, provides another means of representing hardening behavior of metals under cyclic loadings. This basic hardening law is credited to Prager (1956) with further improvements by Ziegler (1959). Then, a combination of kinematic hardening and isotropic hardening, called mixed-hardening, has been pointed out by Hodge (1957). For this case the yield surface can expand and translate simultaneously in stress space, but still remains its original shape. Within this type hardening mechanism, the different degree of experimentally observed Bauschinger effect can be simulated by suitably adjusting these two hardening components.

These conventional models have been used extensively in many engineering applications due to their analytical tractability (see, e.g., Liu, 1997, 2000, 2002). However, they are often too simple to give acceptable approximation to real systems. For example, Fig. 1 shows the cyclic stress–strain curves of the perfectly elastoplastic system, of the bilinear elastoplastic system and of the mixed-hardening elastoplastic system, under the same input of piecewise increasing strain amplitudes. Obviously, all these curves are "over square" near to the elastoplastic transition points, and none of them can meet the basic requirements for cyclic plasticity models (see, e.g., Drucker and Palgen, 1981; Dafalias, 1984). Indeed, as pointed out by many researchers, e.g. Hashiguchi (1993), that the conventional model has serious drawbacks as follows: It is unable to describe the smooth transition from elastic phase to plastic phase, which is observed experimentally for most metals, and instead, an abrupt transition is predicted. It cannot describe the accumulation of plastic deformation such as mechanical ratcheting phenomenon under a constant stress amplitude.

For the conventional theory is far from being able to predict experimental results on real metals, especially under cyclic loading conditions, some modifications have to be made to improve the conventional theory. The unconventional elastoplastic constitutive models, which exclude the above-mentioned assumption in the conventional theory, have been studied, and various models have been proposed since 1960s. For example, an extension of the kinematic hardening model so as to describe even a plastic deformation proceeding in the transition from elastic phase to the normal-yield phase has been attempted by Mróz (1967, 1969) and Iwan (1967) independently. Their extended model, subyield surfaces encircled by a normal-yield surface, has been called a "multi-surface model". Thereafter, based on them, a simplified model employing a normal-yield surface and only one subyield surface enclosing a purely elastic domain

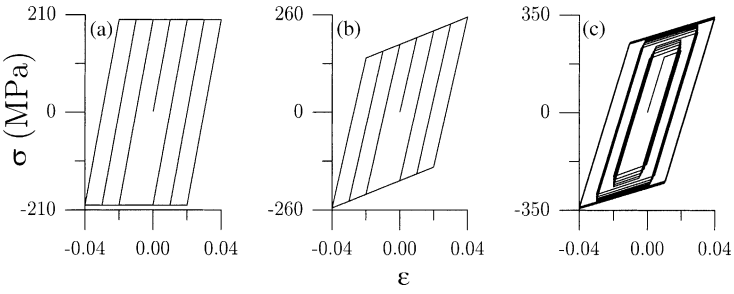

Fig. 1. The hysteretical loops for (a) perfectly elastoplastic model, (b) bilinear elastoplastic model and (c) mixed-hardening elastoplastic model, are all over square near to the elastoplastic transition points.

has been formulated by Dafalias and Popov (1975, 1976), Krieg (1975), Mróz et al. (1979) and Hashiguchi (1988), which has been called a "two surface model". In the plural surfaces theory, we also mention the infinite surface model developed by Mróz et al. (1981), and the subloading surface model developed by Hashiguchi (1989). In terms of mechanical requirements for cyclic plasticity, the condition of continuity in the large and in the small and the Masing effect, Hashiguchi (1993) has examined those models in detail. Chaboche and Rousselier (1983) showed equivalence between the nonlinear kinematic hardening rule of Armstrong and Frederick (1966) and a simple two surface model based on bounding and yield surfaces. Such similarity study may facilitate us to understand and to further develop material models. A detailed discussion concerning multi-surface model, two surface model and the nonlinear kinematic hardening model was given by Chaboche (1986). We just merely and briefly sketch a few progress about cyclic plasticity models which may be to some extent related to our work in the present paper. For further discussion concerning the development of cyclic plasticity before 1990 the interested readers are referred to the paper by Ohno (1990) and the references therein.

In this paper we first concern with one-dimensional models that can be used to describe nonlinear cyclically hysteretical stress–strain behavior through a critical modification. Then, we extend the basic idea to modify a multi-dimensional mixed-hardening model. Instead of zero-measure yield surface for conventional model, the new model obtained by a critical modification of the conventional model allows plasticity to happen in a non-zero-measure yield volume in stress space, which makes the new model exhibiting smooth elastoplastic transition and is able to simulate some cyclic stress–strain behavior. In Drucker's sense we may categorize the new models developed here into unconventional type. However, the new models even allow plasticity to happen inside the yield surface, but they do not need any inner surfaces to delineate the current stress point in plastic state. More importantly, because the new models add only one additional material constant of smoothing factor on their formulations, they are simpler in theoretical and also in practical than other unconventional models.

There have several models that can produce smooth elastoplastic transition, for example, the multi-layer model (Besseling, 1958), the distributed-element model (Iwan, 1966), the Bouc–Wen model (Wen, 1976), the Masing model (see, e.g., Chiang, 1999), the multi-back stress model (Chaboche, 1991), and some nonlinear kinematic hardening models and generalized plasticity models as discussed by Auricchio and Taylor (1995). However, we approach this issue by utilizing a very different, simple yet effective method to modify the original non-smooth elastoplastic model to a smooth one. As will be confident, the proposed method makes the new model revealing drastically different behavior and having largely improved simulation capability than the original model.

2. Modification of one-dimensional perfectly elastoplastic model

2.1. The original model

The following postulations are usually employed to depict the stress–strain relation for one-dimensional perfectly elastoplastic model (see, e.g., Hong and Liu, 1997; Liu, 2000):

$$\dot{\varepsilon} = \dot{\varepsilon}^{\mathrm{e}} + \dot{\varepsilon}^{\mathrm{p}}, \tag{1}$$

$$\dot{\sigma} = E\dot{\varepsilon}^{\mathrm{e}}, \tag{2}$$

$$\dot{\lambda}\sigma = \sigma_{\mathrm{y}}^{0}\dot{\varepsilon}^{\mathrm{p}}, \tag{3}$$

$$|\sigma| \leqslant \sigma_{\mathrm{y}}^{0}, \tag{4}$$

$$\dot{\lambda} \geqslant 0, \tag{5}$$

$$|\sigma|\dot{\lambda} = \sigma_y^0 \dot{\lambda}. \tag{6}$$

The two constants, namely the Young modulus E and the tensile yield stress σ_y^0, are assumed to be positive. Here $\dot{\varepsilon}$, $\dot{\varepsilon}^e$, $\dot{\varepsilon}^p$ and $\dot{\sigma}$ are, respectively, the strain, elastic strain, plastic strain and stress; $\dot{\lambda}$ is a scalar evaluated by $\dot{\lambda}(t) = \int_0^t |\dot{\varepsilon}^p(\xi)| \, d\xi$.

Combining Eqs. (1)–(3), we have

$$\dot{\sigma} + \frac{E}{\sigma_y^0} \dot{\lambda} \sigma = E\dot{\varepsilon}, \tag{7}$$

which together with the complementary trios (4)–(6) enable the model to possess the elastic–plastic switching criteria as follows:

$$\dot{\lambda} = \frac{1}{\sigma_y^0} \sigma\dot{\varepsilon} > 0 \quad \text{if } |\sigma| = \sigma_y^0 \quad \text{and} \quad \sigma\dot{\varepsilon} > 0, \tag{8}$$

$$\dot{\lambda} = 0 \quad \text{if } |\sigma| < \sigma_y^0 \quad \text{or} \quad \sigma\dot{\varepsilon} \leqslant 0. \tag{9}$$

According to the complementary trios (4)–(6), there are just two *phases*: (i) $\dot{\lambda} > 0$ and $|\sigma| = \sigma_y^0$ and (ii) $\dot{\lambda} = 0$ and $|\sigma| \leqslant \sigma_y^0$. From the criteria (8) and (9) it is clear that (i) corresponds to the *plastic phase* while (ii) to the *elastic phase*.

Theorem 1. *For the one-dimensional perfectly elastoplastic model* (1)–(6) *the switch-on strain is given by*

$$\varepsilon_{on} = \varepsilon_{off} + \frac{\sigma_y^0 \mathrm{sgn}(\dot{\varepsilon}) - \sigma_{off}}{E}, \tag{10}$$

where sgn is the signum function.

Proof. For an admissible initial stress $\sigma_{off} := \sigma(t_{off})$ specified at a time $t = t_{off}$, [1] we first integrate Eq. (2) from t_{off} to t with its $\dot{\varepsilon}^e$ replaced by $\dot{\varepsilon}$ due to $\dot{\varepsilon}^p = 0$ in Eq. (1), giving

$$\sigma = \sigma_{off} + E(\varepsilon - \varepsilon_{off}), \tag{11}$$

where $\varepsilon_{off} := \varepsilon(t_{off})$. Then, inserting it into the yield condition $\sigma^2 = (\sigma_y^0)^2$ generates the following equation for ε:

$$E^2(\varepsilon - \varepsilon_{off})^2 + 2E\sigma_{off}(\varepsilon - \varepsilon_{off}) + \sigma_{off}^2 - (\sigma_y^0)^2 = 0. \tag{12}$$

Solving this equation for ε we thus show that the switch-on strain ε_{on} is given by Eq. (10). □

2.2. A critical modification

Now we propose a new model modified from the above perfectly elastoplastic model, which provides a quite significant improvement in describing stress–strain behavior to avoid some major defects of the original model. In order to alleviate the non-smoothness of the stress–strain curves for perfectly elastoplastic model as shown in Fig. 1(a) we propose, instead of the constant yield stress σ_y^0, a modified piecewise-constant yield stress given as follows:

[1] t_{off} may be an initial time in the elastic phase or the latest time for the occurrence of unloading.

$$\sigma_{\mathrm{y}}^{m} := \frac{\sigma_{\mathrm{y}}^{0} + (\rho - 1)\sigma_{\mathrm{off}}\mathrm{sgn}(\dot{\varepsilon})}{\rho}. \tag{13}$$

The above σ_{off} is the stress at the latest unloading point; initially we may let $\sigma_{\mathrm{off}} = 0$. The smoothing factor $\rho > 1$ is a material constant determined by experimental test. When $\rho = 1$, $\sigma_{\mathrm{y}}^{m} = \sigma_{\mathrm{y}}^{0}$ and we recover to the original non-smooth model.

Now we prove the following two important results.

Theorem 2. *If $1 < \rho \leqslant 2$, the switch-on strain for the newly modified one-dimensional perfectly elastoplastic model is given by*

$$\varepsilon_{\mathrm{on}} = \varepsilon_{\mathrm{off}} + \frac{\sigma_{\mathrm{y}}^{0}\mathrm{sgn}(\dot{\varepsilon}) - \sigma_{\mathrm{off}}}{\rho E}. \tag{14}$$

Proof. At first we need ρ to be in the range of $1 < \rho \leqslant 2$; otherwise, for some extremal cases of σ_{off} very near to $\pm\sigma_{\mathrm{y}}^{0}$ we may obtain negative σ_{y}^{m} from Eq. (13). For admissible initial stress [2] σ_{off} specified at time $t = t_{\mathrm{off}}$, substituting the elastic equation (11) into the new yield condition $\sigma^2 = (\sigma_{\mathrm{y}}^{m})^2$ generates the following equation for ε:

$$E^2(\varepsilon - \varepsilon_{\mathrm{off}})^2 + 2E\sigma_{\mathrm{off}}(\varepsilon - \varepsilon_{\mathrm{off}}) + \sigma_{\mathrm{off}}^2 - (\sigma_{\mathrm{y}}^{m})^2 = 0. \tag{15}$$

Substituting Eq. (13) for σ_{y}^{m} into the above equation and solving it for ε we obtain the result in Eq. (14). □

The specification of the new σ_{y}^{m} to be a subyield stress is equivalent to shorten the original switching-on strain given by Eq. (10) to that given by Eq. (14) with a factor $\rho > 1$.

Theorem 3. *The modified yield stress σ_{y}^{m} satisfies the following inequality*

$$0 < \sigma_{\mathrm{y}}^{m} < \sigma_{\mathrm{y}}^{0}. \tag{16}$$

Proof. Because of $1 < \rho \leqslant 2$ and $|\sigma_{\mathrm{off}}| < \sigma_{\mathrm{y}}^{0}$ the above inequality follows from Eq. (13) directly. □

We should note that σ_{y}^{m} cannot be a constant for all time; otherwise, Eq. (15) may has no solution for some cases. The strategy employed in the new model amounts to modify the $\dot{\lambda}$ in Eq. (7) subjected to the new switching criteria:

$$\dot{\lambda} = \frac{1}{\sigma_{\mathrm{y}}^{0}}\sigma\dot{\varepsilon} > 0 \quad \text{if } \sigma_{\mathrm{y}}^{0} > |\sigma| \geqslant \sigma_{\mathrm{y}}^{m} \quad \text{and} \quad \sigma\dot{\varepsilon} > 0, \tag{17}$$

$$\dot{\lambda} = 0 \quad \text{if } |\sigma| < \sigma_{\mathrm{y}}^{m} \quad \text{or} \quad \sigma\dot{\varepsilon} \leqslant 0. \tag{18}$$

It admits plasticity occurring in a finite stress interval of $\sigma_{\mathrm{y}}^{m} \leqslant |\sigma| < \sigma_{\mathrm{y}}^{0}$. The original yield points $|\sigma| = \sigma_{\mathrm{y}}^{0}$ can be viewed mathematically as limiting points, and $|\sigma| \geqslant \sigma_{\mathrm{y}}^{0}$ is not permitted in the new model. As the original model is, the new model is thermodynamically consistent since $\dot{\lambda} > 0$ in the plastic phase and $\dot{\lambda} = 0$ in the elastic phase as shown in Eqs. (17) and (18).

[2] Instead of $|\sigma| \leqslant \sigma_{\mathrm{y}}^{0}$ for the original model, for the new model we call σ admissible if $|\sigma| < \sigma_{\mathrm{y}}^{0}$.

2.3. Smooth stress–strain curves

From Eqs. (7) and (17) we have

$$\dot{\sigma} = E\dot{\varepsilon}\left(1 - \frac{\sigma^2}{(\sigma_y^0)^2}\right) \tag{19}$$

in the plastic phase. Because we allow plasticity to happen when σ^2 lies in the range of $(\sigma_y^0)^2 > \sigma^2 \geqslant (\sigma_y^m)^2$, the above right-hand side is not equal to zero, which is different from that for the original model, of which the above right-hand side is zero because plasticity is permitted only in the zero-measure two points set of $\sigma = \pm\sigma_y^0$. Let us further note four important points: (a) For the modified model we do not care the consistency condition, because yield surface has been replaced by a new concept of yield volume whose measure is not zero in stress space; however, $\dot{\lambda}$ for the new model is same as that for the original perfectly elastoplastic model which is obtained by the consistency condition. (b) From Eq. (19) follows two fixed points $\sigma = \sigma_y^0$ and $\sigma = -\sigma_y^0$. They are the attracting points of the new model dynamics. (c) Hence, for the new model it is obvious that extensive plastic loading overwhelms and wipes out memory many, if not all, of the past effect. No matter how many cycles the modeled material has experienced, its stress–strain curve will approach to one of the two bounding lines, $\sigma = \pm\sigma_y^0$, if plastic deformation goes on extensively in one of the two directions. (d) The new model allows stress control in the range of $|\sigma| < \sigma_y^0$; this is however impossible for the original perfectly elastoplastic model.

If we view σ as a function of ε, Eq. (19) can be written as

$$\frac{\mathrm{d}\sigma}{\mathrm{d}\varepsilon} = E\left(1 - \frac{\sigma^2}{(\sigma_y^0)^2}\right). \tag{20}$$

Integrating the above equation with some algebraic manipulations gives

$$\frac{\sigma(t)}{\sigma_y^0} = \frac{[\sigma(t_i) + \sigma_y^0]\exp\left\{\frac{2E[\varepsilon(t)-\varepsilon(t_i)]}{\sigma_y^0}\right\} + \sigma(t_i) - \sigma_y^0}{[\sigma(t_i) + \sigma_y^0]\exp\left\{\frac{2E[\varepsilon(t)-\varepsilon(t_i)]}{\sigma_y^0}\right\} + \sigma_y^0 - \sigma(t_i)}, \tag{21}$$

where t_i can be a switched-on time. In the new model we do allow $|\sigma(t_i)| < \sigma_y^0$ but not allow $|\sigma(t_i)| = \sigma_y^0$; for the former case it is obvious that $|\sigma(t)| < \sigma_y^0$ for all $t \geqslant t_i$, but for the latter case it is obvious that $|\sigma(t)| = \sigma_y^0$ for all $t \geqslant t_i$, which thus leads to a plastic plateau and a non-smooth elastoplastic transition. Under monotonically straining it is obvious that $|\sigma(t)|$ approaches to σ_y^0, and hence the points of $|\sigma| = \sigma_y^0$ are limiting points.

In order to get a clear picture about the stress–strain relations for the new model, we apply Eqs. (11) and (21) to calculate the stresses in elastic phase and in plastic phase, respectively, by letting ε to be the control input, and we use Eq. (14) to determine the switching-on strain. The Young modulus $E = 20\,000$ MPa was taken, and the modified initial yield stress $\sigma_y^m = \sigma_y^0/\rho = 200$ MPa was fixed in all calculations. Fig. 2 displays the monotonic stress–strain curves for different ρ's and σ_y^0's as shown in the figure, where we select the two constants of ρ and σ_y^0 so as to make the five curves have the same initial yield point $(\sigma, \varepsilon) = (200\ \text{MPa}, 0.01)$. Obviously, stress runs in the range of $(\sigma_y^0/\rho, \sigma_y^0)$ after initially yielding, [3] and each stress–strain curve tends to its limiting value σ_y^0 for large strain. It can be seen that more larger ρ leads to more strain hardening and also more smooth transition from elasticity to plasticity, and when $\rho = 1$ we recover to the relation for the perfectly elastoplastic model.

[3] For the new model, the smoothing factor ρ has a natural mechanical meaning if we view σ_y^0/ρ as initial yield stress and σ_y^0 as limiting strength.

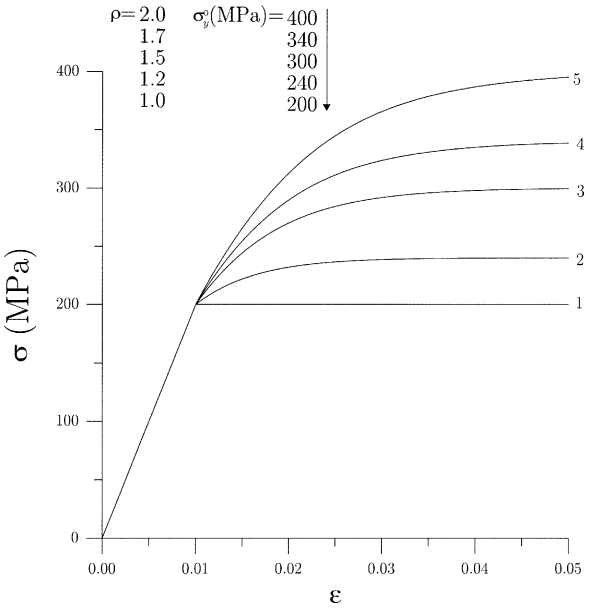

Fig. 2. The monotonic stress–strain curves for different smooth factors and yield stresses.

If we view σ^2 as a function of λ, Eq. (19), after multiplying by σ on both sides and inserting Eq. (17) for $\sigma\dot{\varepsilon}$, becomes

$$\frac{\mathrm{d}\sigma^2}{\mathrm{d}\lambda}+\frac{2E}{\sigma_{\mathrm{y}}^0}\sigma^2=2E\sigma_{\mathrm{y}}^0. \tag{22}$$

Integrating the above equation gives

$$\sigma^2=(\sigma_{\mathrm{y}}^m)^2+\left[(\sigma_{\mathrm{y}}^0)^2-(\sigma_{\mathrm{y}}^m)^2\right]\left[1-\exp\left(\frac{-2E\lambda}{\sigma_{\mathrm{y}}^0}\right)\right], \tag{23}$$

where at $\lambda=0$ we let $\sigma^2=(\sigma_{\mathrm{y}}^m)^2$. The above result is quite significant, which says that for the new model in each plastic phase the modeled material can harden from an initial yield strength σ_{y}^m to a saturated strength σ_{y}^0 with a strain-hardening rate $2E/\sigma_{\mathrm{y}}^0$. Very interestingly, the new model possesses a natural hardening mechanism as specified by Eq. (23), which is different from the standard saturation type hardening law as to be given in Eq. (59). This is however impossible for the original model, of which the hardening term disappears.

In Fig. 3(a)–(d) we give some cyclic stress–strain curves for different ρ's and σ_{y}^0's as listed in Table 1, under the input of piecewise increasing amplitudes of strain with each strain amplitude being applied five cycles. They show that the modified model is able to reveal smooth elastoplastic transition, strain hardening, the Bauschinger effect, as well as a little cyclic hardening effect in small strain range. However, for this simple modified model the hysteretical loops are stabilized rapidly to a single loop within one cycle for each strain amplitude. In order to simulate cyclic hardening in a more feasible way we need to supplement mixed-hardening effect into the model as that to be investigated in Section 4. In Fig. 3(e) the time histories of the modified yield stresses σ_{y}^m's for different ρ's are plotted.

About ρ and σ_{y}^m there have at least three important points deserving to note: (a) For smaller ρ there has smaller stress range that the material can harden, and such that σ_{y}^m varies in a very narrow range. For

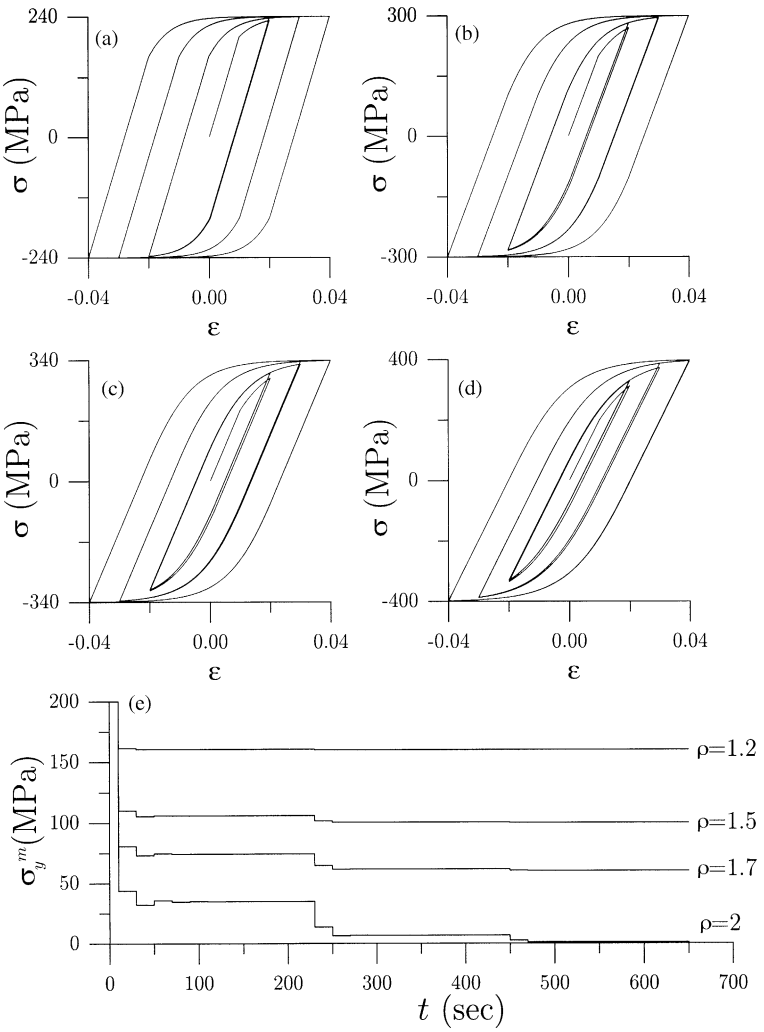

Fig. 3. The hysteretical loops for the modified perfectly elastoplastic model with different smooth factors and yield stresses. The modification renders the new model having more smooth elastoplastic transition. The last one plot shows the time histories of the modified yield stresses.

Table 1
Material constants used in Figs. 1, 3, 5, 6

E (MPa)	σ_y^0 (MPa)	ρ		E_b (MPa)		σ_y^u (MPa)	n	
20 000	200	1	Fig. 1(a)	2000	Fig. 1(b)	300	5	Fig. 1(c)
20 000	240	1.2	Fig. 3(a)	2000	Fig. 5(a)	340	5	Fig. 6(a)
20 000	300	1.5	Fig. 3(b)	2000	Fig. 5(b)	400	5	Fig. 6(b)
20 000	340	1.7	Fig. 3(c)	2000	Fig. 5(c)	440	5	Fig. 6(c)
20 000	400	2	Fig. 3(d)	2000	Fig. 5(d)	500	5	Fig. 6(d)

example, after the first cycle in Fig. 3(e) for the case $\rho = 1.2$, σ_y^m is almost tended to a constant value. But in the first cycle σ_y^m as can be seen experiences a large jump from 200 MPa to about 160 MPa, because the

material rapidly hardens in the first cycle, and after that the cyclic hardening almost stops. (b) More larger ρ gives more smaller σ_y^m, and hence more smooth elastoplastic transition. (c) The time histories of σ_y^m as shown in Fig. 3(e) tell us that σ_y^m decreases to certain small value when strain amplitude increases. For example for the case $\rho = 2$, σ_y^m almost tends to zero value at the last few cycles, which renders stress–strain curve almost being $\mathbb{C}^1$ smooth at the elastoplastic transition points.

In this occasion let us give one comment on the basic mechanical requirement of continuity in the large, i.e., $\mathbb{C}^1$ smooth stress–strain curve, that Hashiguchi (1993) proposed to assess the smoothness of elastoplastic constitutive models. This requirement needs the material model responding plastically under a loading process even starting immediately from a zero stress state. That is, elastic domain is shrinking to a zero stress point. This is however not true for most metals being loaded from their annealed state. As remarked by Hashiguchi (1993) only very few models that can meet this stringent requirement. In personal view, it is a mathematical requirement rather than a mechanical requirement for modeling material behavior.

In order to display the strain ratcheting effect that the new model can simulate, we may conversely employ σ as the control input and calculate ε by the following equation

$$\varepsilon(t) = \varepsilon(t_i) + \frac{\sigma_y^0}{2E} \ln \frac{[\sigma_y^0 + \sigma(t)][\sigma_y^0 - \sigma(t_i)]}{[\sigma_y^0 - \sigma(t)][\sigma_y^0 + \sigma(t_i)]} \tag{24}$$

in the plastic phase, and by Eq. (11) in the elastic phase. The switching-on stress is determined by

$$\sigma_{on} = \frac{\sigma_y^0 \mathrm{sgn}(\dot{\sigma})}{\rho}. \tag{25}$$

In Fig. 4(a)–(h) with stress being input we show some cyclic stress–strain curves for different initial prestresses $\sigma(t_i)$'s but with $\sigma_y^0 = 400$ MPa and $\rho = 2$ being kept constant for all cases. They show that the modified model is able to reveal ratcheting behavior, and we can see that more larger mean value of stress leads to more larger strain ratcheting, and that zero mean stress induces no strain ratcheting. These results are at least qualitatively consistent with the experimental observations for most metals.

3. Modification of one-dimensional bilinear elastoplastic model

Although the above modified model can describe a little Bauschinger effect, in order to enhance the simulation capability it needs the model able to describe kinematic hardening more and more. In many metals subjected to cyclic loading, it is experimentally observed that the center of yield surface experiences a motion in the direction of plastic flow. This hardening behavior is known as the Bauschinger effect. Dafalias (1984) has experimentally observed that the reverse yielding initiates before even the tensile stress changes to compressive for grade 60 steel.

A simple phenomenological description that captures the Bauschinger effect is constructed by introducing an additional internal variable called back stress in the formulation, which defines the location of the center of the yield surface. Then, Eqs. (1)–(6) are extended to the following one-dimensional bilinear elastoplastic model (see, e.g., Liu, 1997, 2000; Hong and Liu, 1999):

$$\dot{\varepsilon} = \dot{\varepsilon}^e + \dot{\varepsilon}^p, \tag{26}$$

$$\sigma = \sigma^a + \sigma^b, \tag{27}$$

$$\dot{\sigma} = E\dot{\varepsilon}^e, \tag{28}$$

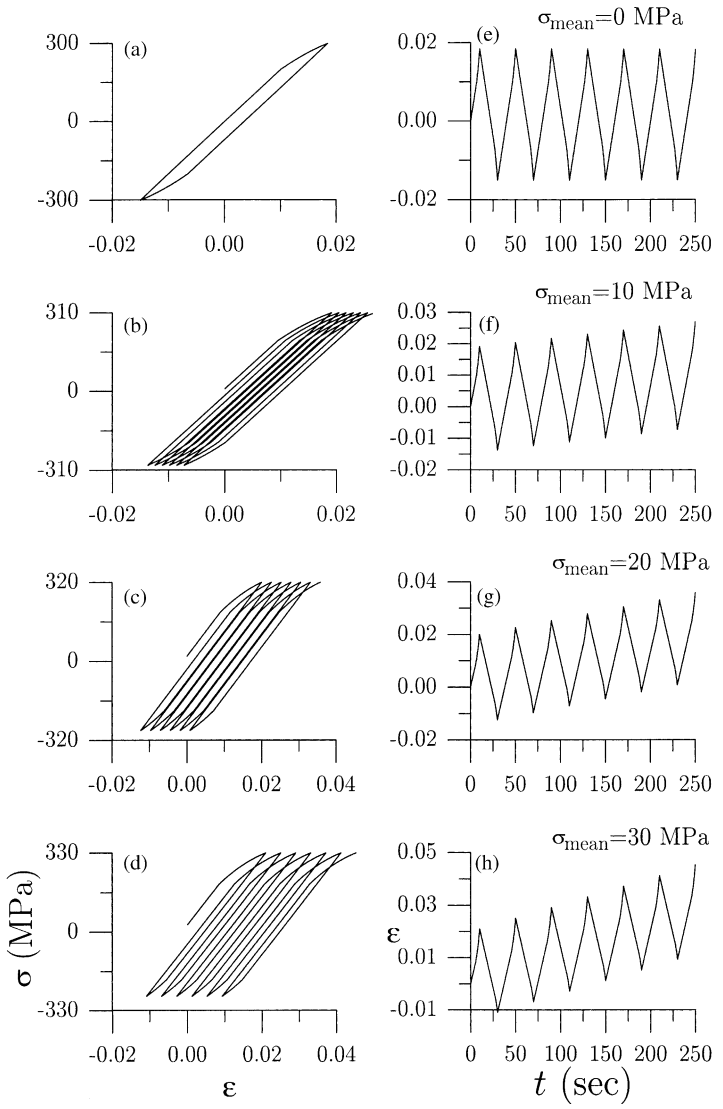

Fig. 4. Under constant amplitude stress control the strain ratcheting behavior for the modified perfectly elastoplastic model is shown for different mean stresses. More larger mean stress renders more larger strain ratcheting.

$$\dot{\lambda}\sigma^{\mathrm{a}} = \sigma_{\mathrm{y}}^{0}\dot{\varepsilon}^{\mathrm{p}}, \tag{29}$$

$$\dot{\sigma}^{\mathrm{b}} = E_{\mathrm{b}}\dot{\varepsilon}^{\mathrm{p}}, \tag{30}$$

$$|\sigma^{\mathrm{a}}| \leqslant \sigma_{\mathrm{y}}^{0}, \tag{31}$$

$$\dot{\lambda} \geqslant 0, \tag{32}$$

$$|\sigma^{\mathrm{a}}|\dot{\lambda} = \sigma_{\mathrm{y}}^{0}\dot{\lambda}. \tag{33}$$

From Eqs. (26)–(28), (30) it follows that

$$\frac{1}{E}\dot{\sigma} + \frac{1}{E_b}(\dot{\sigma} - \dot{\sigma}^a) = \dot{\varepsilon}, \tag{34}$$

$$\frac{1}{E}(\dot{\sigma}^a + \dot{\sigma}^b) + \frac{1}{E_b}\dot{\sigma}^b = \dot{\varepsilon}, \tag{35}$$

$$\dot{\sigma}^a + E_b\dot{\varepsilon}^p = E(\dot{\varepsilon} - \dot{\varepsilon}^p). \tag{36}$$

By integrating the above three equations from t_i to t we immediately obtain

$$\sigma(t) = \sigma(t_i) + \beta[\sigma^a(t) - \sigma^a(t_i)] + \beta E_b[\varepsilon(t) - \varepsilon(t_i)], \tag{37}$$

$$\sigma^b(t) = \sigma^b(t_i) + \alpha[\sigma^a(t_i) - \sigma^a(t)] + \beta E_b[\varepsilon(t) - \varepsilon(t_i)], \tag{38}$$

$$\varepsilon^p(t) = \varepsilon^p(t_i) + \frac{1}{E + E_b}[\sigma^a(t_i) - \sigma^a(t)] + \beta[\varepsilon(t) - \varepsilon(t_i)], \tag{39}$$

where the parameter β is defined by

$$\beta := \frac{E}{E + E_b} \tag{40}$$

and

$$\alpha := 1 - \beta = \frac{E_b}{E + E_b} \tag{41}$$

is the modulus ratio, because $\alpha E = \beta E_b$ is the post-yield modulus.

Formulae (37)–(39) indicate that stress, back stress and plastic strain are linear functions of strain, active stress and some related initial values $\varepsilon^p(t_i)$, $\varepsilon(t_i)$, $\sigma^a(t_i)$, $\sigma^b(t_i)$ and $\sigma(t_i)$, the latter three of which are however not linearly independent, since they are related by $\sigma(t_i) = \sigma^a(t_i) + \sigma^b(t_i)$. Hence, if we know $\sigma^a(t)$, the other three quantities $\sigma(t)$, $\sigma^b(t)$ and $\varepsilon^p(t)$ can be calculated immediately.

Inserting the flow rule (29) for $\dot{\varepsilon}^p$ into Eq. (36) we find that the active stress is governed by

$$\dot{\sigma}^a + \frac{E + E_b}{\sigma_y^0}\dot{\lambda}\sigma^a = E\dot{\varepsilon}, \tag{42}$$

where $\dot{\lambda}$ is subjected to the following switching criteria:

$$\dot{\lambda} = \frac{\beta}{\sigma_y^0}\sigma^a\dot{\varepsilon} > 0 \quad \text{if } \sigma_y^0 > |\sigma^a| \geqslant \sigma_y^m \quad \text{and} \quad \sigma^a\dot{\varepsilon} > 0, \tag{43}$$

$$\dot{\lambda} = 0 \quad \text{if } |\sigma^a| < \sigma_y^m \quad \text{or} \quad \sigma^a\dot{\varepsilon} \leqslant 0. \tag{44}$$

The above modified yield stress, analogous to the one in Eq. (13), is now given as follows:

$$\sigma_y^m := \frac{\sigma_y^0 + (\rho - 1)\sigma_{off}^a \mathrm{sgn}(\dot{\varepsilon})}{\rho}, \tag{45}$$

where σ_{off}^a is the active stress at the latest unloading point.

Similarly, we can prove the following result.

Theorem 4. *If* $1 < \rho \leqslant 2$, *the switch-on strain for the newly modified one-dimensional bilinear elastoplastic model is given by*

$$\varepsilon_{\text{on}} = \varepsilon_{\text{off}} + \frac{\sigma_{\text{y}}^0 \text{sgn}(\dot{\varepsilon}) - \sigma_{\text{off}}^{\text{a}}}{\rho E}. \tag{46}$$

From Eqs. (42) and (43) we obtain

$$\frac{\text{d}\sigma^{\text{a}}}{\text{d}\varepsilon} = E\left(1 - \frac{(\sigma^{\text{a}})^2}{(\sigma_{\text{y}}^0)^2}\right). \tag{47}$$

Integrating the above equation gives

$$\frac{\sigma^{\text{a}}(t)}{\sigma_{\text{y}}^0} = \frac{[\sigma^{\text{a}}(t_i) + \sigma_{\text{y}}^0] \exp\left\{\frac{2E[\varepsilon(t)-\varepsilon(t_i)]}{\sigma_{\text{y}}^0}\right\} + \sigma^{\text{a}}(t_i) - \sigma_{\text{y}}^0}{[\sigma^{\text{a}}(t_i) + \sigma_{\text{y}}^0] \exp\left\{\frac{2E[\varepsilon(t)-\varepsilon(t_i)]}{\sigma_{\text{y}}^0}\right\} + \sigma_{\text{y}}^0 - \sigma^{\text{a}}(t_i)}, \tag{48}$$

where t_i can be chosen to be the switched-on time. In the new model we allow $|\sigma^{\text{a}}(t_i)| < \sigma_{\text{y}}^0$ and not allow $|\sigma^{\text{a}}(t_i)| = \sigma_{\text{y}}^0$; for the former case it is obvious that $|\sigma^{\text{a}}(t)| < \sigma_{\text{y}}^0$ for all $t \geqslant t_i$, and for the latter case it is obvious that $|\sigma^{\text{a}}(t)| = \sigma_{\text{y}}^0$ for all $t \geqslant t_i$, which thus leads to a non-smooth elastoplastic transition. Under monotonically straining it is obvious that $|\sigma^{\text{a}}(t)|$ approaches to σ_{y}^0, and hence the points of $|\sigma^{\text{a}}| = \sigma_{\text{y}}^0$ are limiting points of σ^{a}.

Now, we apply Eqs. (48) and (37)–(39) to calculate the responses in plastic phase by letting ε to be the control input, and use Eq. (46) to determine the switching-on strain. In Fig. 5(a)–(d) we give some cyclic stress–strain curves for different ρ's and σ_{y}^0's and fixed E_{b} as listed in Table 1. They show that the modified model is able to reveal smooth elastoplastic transition, strain hardening and strong Bauschinger effect, which shows that reverse yielding initiating before even the tensile stress changes to compressive. The hysteretical loops are stabilized very soon within one cycle for each strain amplitude. However, the experimental observations for most metals do not support this type behavior. Therefore, we need to consider a more reasonable model of mixed-hardening and its modification as follows.

4. Modification of one-dimensional mixed-hardening elastoplastic model

The third model that we attempt to modify is one-dimensional mixed-hardening elastoplastic model, which allows the yield surface to expand and to translate simultaneously in stress space, and is obtained from Eqs. (26)–(33) by letting the yield stress σ_{y} depend on λ, that is, $\sigma_{\text{y}} = \sigma_{\text{y}}(\lambda)$.

With this in mind, from Eqs. (26)–(30) it follows that

$$\dot{\sigma}^{\text{a}} + \frac{E + E_{\text{b}}}{\sigma_{\text{y}}} \dot{\lambda} \sigma^{\text{a}} = E\dot{\varepsilon}. \tag{49}$$

The product of σ^{a} with the above equation is

$$\sigma^{\text{a}}\dot{\sigma}^{\text{a}} + \frac{E + E_{\text{b}}}{\sigma_{\text{y}}} \dot{\lambda} (\sigma^{\text{a}})^2 = E\sigma^{\text{a}}\dot{\varepsilon}, \tag{50}$$

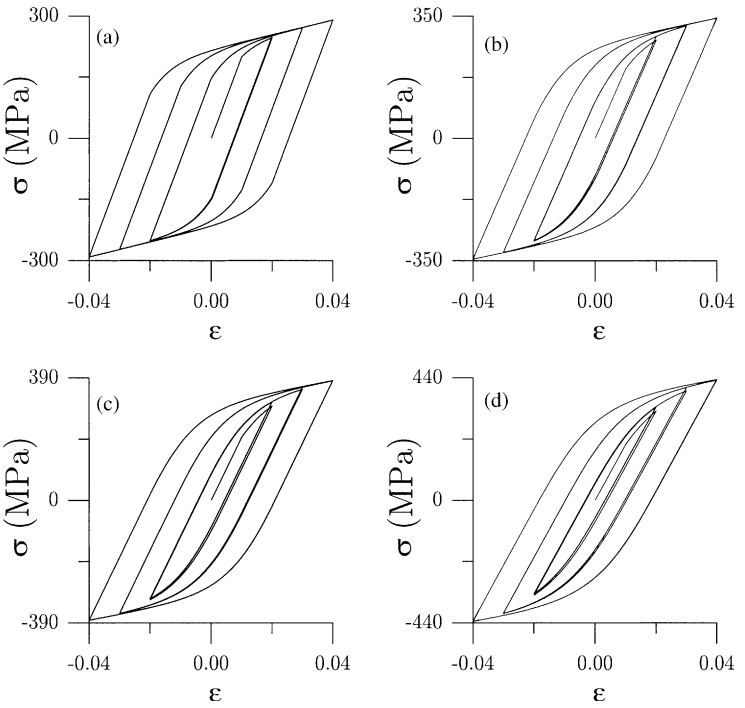

Fig. 5. The hysteretical loops for the modified bilinear elastoplastic model with different smooth factors and yield stresses. The modification renders the new model having more smooth elastoplastic transition.

which, due to $(\sigma^{\mathrm{a}})^2 = \sigma_{\mathrm{y}}^2$ at yielding point and $\sigma_{\mathrm{y}} = \sigma_{\mathrm{y}}(\lambda)$, furnishes the following switching criteria:

$$\dot{\lambda} = \frac{E}{(E + E_{\mathrm{b}} + \sigma_{\mathrm{y}}')\sigma_{\mathrm{y}}}\sigma^{\mathrm{a}}\dot{\varepsilon} > 0 \quad \text{if } |\sigma^{\mathrm{a}}| = \sigma_{\mathrm{y}} \text{ and } \sigma^{\mathrm{a}}\dot{\varepsilon} > 0, \tag{51}$$

$$\dot{\lambda} = 0 \quad \text{if } |\sigma^{\mathrm{a}}| < \sigma_{\mathrm{y}} \text{ or } \sigma^{\mathrm{a}}\dot{\varepsilon} \leqslant 0. \tag{52}$$

In above σ_{y}' denotes the differentiation of $\sigma_{\mathrm{y}} = \sigma_{\mathrm{y}}(\lambda)$ with respect to λ.

Eq. (49) together with the switching criteria (51) and (52) are the governing equations for the conventional one-dimensional mixed-hardening elastoplastic model. Now we subject $\dot{\lambda}$ to the new switching criteria:

$$\dot{\lambda} = \frac{E}{(E + E_{\mathrm{b}} + \sigma_{\mathrm{y}}')\sigma_{\mathrm{y}}}\sigma^{\mathrm{a}}\dot{\varepsilon} > 0 \quad \text{if } \sigma_{\mathrm{y}} > |\sigma^{\mathrm{a}}| \geqslant \sigma_{\mathrm{y}}^m \quad \text{and} \quad \sigma^{\mathrm{a}}\dot{\varepsilon} > 0, \tag{53}$$

$$\dot{\lambda} = 0 \quad \text{if } |\sigma^{\mathrm{a}}| < \sigma_{\mathrm{y}}^m \quad \text{or} \quad \sigma^{\mathrm{a}}\dot{\varepsilon} \leqslant 0, \tag{54}$$

where

$$\sigma_{\mathrm{y}}^m := \frac{\sigma_{\mathrm{y}}(\lambda_{\mathrm{off}}) + (\rho - 1)\sigma_{\mathrm{off}}^{\mathrm{a}}\mathrm{sgn}(\dot{\varepsilon})}{\rho} \tag{55}$$

and λ_{off} and $\sigma_{\mathrm{off}}^{\mathrm{a}}$ are, respectively, the values of λ and σ^{a} at the latest unloading point.

Eq. (49) together with the new switching criteria (53) and (54) are the governing equations for the modified one-dimensional mixed-hardening elastoplastic model, which includes a smoothing factor in the formulation. Substituting Eq. (53) for $\dot{\lambda}$ into Eq. (49) gives a nonlinear equation for σ^{a},

$$\frac{\mathrm{d}\sigma^{\mathrm{a}}}{\mathrm{d}\varepsilon} = E\left(1 - \frac{(E+E_{\mathrm{b}})(\sigma^{\mathrm{a}})^2}{(E+E_{\mathrm{b}}+\sigma'_{\mathrm{y}})\sigma_{\mathrm{y}}^2}\right). \tag{56}$$

However, because of the dependence of σ_{y} on λ, the above equation alone insuffices to determine σ^{a}, which must be supplemented with Eq. (53) of the following form:

$$\frac{\mathrm{d}\lambda}{\mathrm{d}\varepsilon} = \frac{E}{(E+E_{\mathrm{b}}+\sigma'_{\mathrm{y}})\sigma_{\mathrm{y}}}\sigma^{\mathrm{a}}. \tag{57}$$

Here we view strain as input, and the strain to switch-on plasticity is given below.

Theorem 5. *If* $1 < \rho \leqslant 2$, *the switch-on strain for the newly modified one-dimensional mixed-hardening elastoplastic model is given by*

$$\varepsilon_{\mathrm{on}} = \varepsilon_{\mathrm{off}} + \frac{\sigma_{\mathrm{y}}(\lambda_{\mathrm{off}})\mathrm{sgn}(\dot{\varepsilon}) - \sigma^{\mathrm{a}}_{\mathrm{off}}}{\rho E}. \tag{58}$$

Unlike to Eq. (20) for modified one-dimensional perfectly elastoplastic model, and Eq. (47) for modified one-dimensional bilinear elastoplastic model, Eq. (56) cannot be integrated explicitly with a closed-form solution, because $(\sigma^{\mathrm{a}})^2$ is not equal to σ_{y}^2 for the modified one-dimensional mixed-hardening elastoplastic model and because the material function σ_{y} depends on λ. This is also true for the linear isotropic hardening case, i.e., σ'_{y} =constant. Eqs. (56) and (57) are more complicated than the corresponding equations for the original model, which may be solved exactly for the linear hardening case because of $(\sigma^{\mathrm{a}})^2 = \sigma_{\mathrm{y}}^2$. The coupled equations (56) and (57) are then numerically integrated by the group-preserving scheme developed by Liu (2001), and at the same time stress, back stress and plastic strain are calculated, respectively, by Eqs. (37)–(39). In Fig. 6(a)–(d) we give some cyclic stress–strain curves for fixed n and different σ_{y}^0's and σ_{y}^u's within the following isotropic hardening function

$$\sigma_{\mathrm{y}}(\lambda) = \sigma_{\mathrm{y}}^0 + (\sigma_{\mathrm{y}}^u - \sigma_{\mathrm{y}}^0)[1 - \exp(-n\lambda)], \tag{59}$$

where σ_{y}^0 and σ_{y}^u are, respectively, the initial yield stress and the ultimate yield stress, and n is the strain-hardening rate. The material constants used are listed in Table 1. Examining the responses as shown in Fig. 6(a)–(d) for symmetric cyclic loading under piecewise increasing strain amplitudes reveals again that the modified model can smooth stress–strain curves, and strain hardening, cyclic hardening, as well as the Bauschinger effect are evident. For each strain amplitude the peak stress increases with the number of cycles stabilizing at a level which increases with the subsequent strain amplitude for the next set of cycling. This indicates an increase of the elastic region due to isotropic hardening. In Fig. 6(e) the time histories of the modified yield stresses σ_{y}^m's for different ρ's are plotted. More larger ρ gives more smaller σ_{y}^m, which explains the reason that more larger ρ gives more smooth elastoplastic transition. However, for the case $\rho = 1.2$, which is not larger enough to depress the value of σ_{y}^m, the cyclic stress–strain curve as shown in Fig. 6(a) is not so smooth as that for the other three cases.

5. Multi-dimensional mixed-hardening elastoplastic model and its modification

In this section we attempt to extend the above results to the multi-dimensional models. Because the perfectly elastoplastic model and the bilinear elastoplastic model are both special cases of the mixed-hardening elastoplastic model, we skip directly to the multi-dimensional mixed-hardening elastoplastic model, which can be re-formulated as the following postulations (see, e.g., Hong and Liu, 1993; Caddemi, 1994; Auricchio and Beirão da Veiga, 2003):

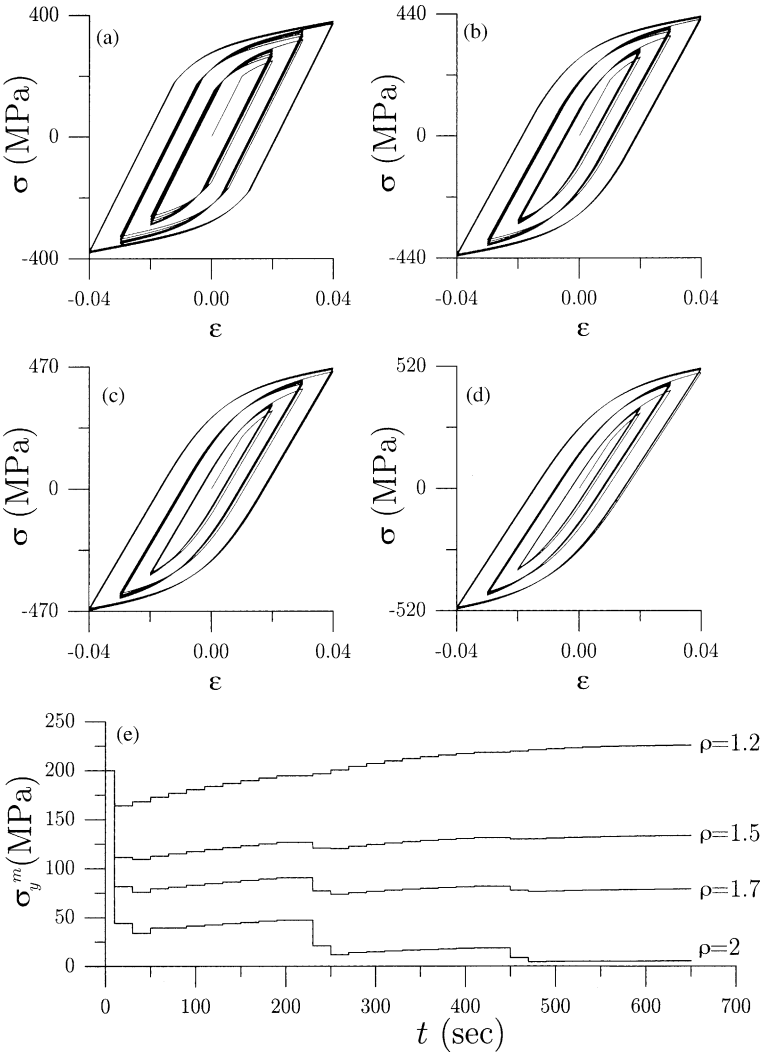

Fig. 6. The hysteretical loops for the modified mixed-hardening elastoplastic model with different ρ's, σ_y^0's and σ_y^u's. The modification renders the new model having more smooth elastoplastic transition. The last one plot shows the time histories of the modified yield stresses.

$$\dot{\mathbf{e}} = \dot{\mathbf{e}}^{\mathrm{e}} + \dot{\mathbf{e}}^{\mathrm{p}}, \tag{60}$$

$$\mathbf{s} = \mathbf{s}_{\mathrm{a}} + \mathbf{s}_{\mathrm{b}}, \tag{61}$$

$$\dot{\mathbf{s}} = 2G\dot{\mathbf{e}}^{\mathrm{e}}, \tag{62}$$

$$\dot{\lambda}\mathbf{s}_{\mathrm{a}} = 2\tau_{\mathrm{y}}\dot{\mathbf{e}}^{\mathrm{p}}, \tag{63}$$

$$\dot{\mathbf{s}}_{\mathrm{b}} = 2k'\dot{\mathbf{e}}^{\mathrm{p}}, \tag{64}$$

$$\|\mathbf{s}_{\mathrm{a}}\| \leqslant \sqrt{2}\tau_{\mathrm{y}}, \tag{65}$$

$$\dot{\lambda} \geqslant 0, \tag{66}$$

$$\|\mathbf{s}_a\|\dot{\lambda} = \sqrt{2}\tau_y\dot{\lambda}. \tag{67}$$

Here the norm of a tensor is defined as $\|\mathbf{s}_a\| := \sqrt{\mathbf{s}_a \cdot \mathbf{s}_a}$ and a dot between two same order tensors denotes their Euclidean inner product.

In the above $\mathbf{e}$, $\mathbf{e}^e$, $\mathbf{e}^p$, $\mathbf{s}$, $\mathbf{s}_a$ and $\mathbf{s}_b$ are, respectively, the deviatoric tensors of strain, elastic strain, plastic strain, stress, active stress and back stress, all symmetric and traceless, whereas λ is a scalar. It is also postulated that with the above differential model there is a time instant designated as $t = t_0$, called the zero-value time, before and at which the material is in the zero-value state in the sense that the relevant values $\mathbf{e}$, $\mathbf{e}^e$, $\mathbf{e}^p$, $\mathbf{s}$, $\mathbf{s}_a$, $\mathbf{s}_b$ and λ are all zero. Here, the shear modulus $G > 0$ is assumed to be a material constant, and the shear yield strength $\tau_y > 0$ and the shear kinematic modulus k' are functions of the equivalent shear plastic strain λ given by

$$\lambda(t) = \int_{t_0}^{t} \sqrt{2}\|\dot{\mathbf{e}}^p(\xi)\|\,\mathrm{d}\xi. \tag{68}$$

The material is further assumed to be weakly stable, Hong and Liu (1993):

$$\tau_y' + k' + G > 0. \tag{69}$$

Here a prime attached to a material function denotes the derivative with respect to its argument, for example, $\tau_y'(\lambda) := \mathrm{d}\tau_y(\lambda)/\mathrm{d}\lambda$.

5.1. Switch of plastic irreversibility

From Eqs. (60)–(64) it follows that

$$\dot{\mathbf{s}}_a + \frac{k' + G}{\tau_y}\dot{\lambda}\mathbf{s}_a = 2G\dot{\mathbf{e}}. \tag{70}$$

Taking the inner product of Eq. (70) with $\mathbf{s}_a$, we get

$$G\mathbf{s}_a \cdot \dot{\mathbf{e}} = (\tau_y' + k' + G)\tau_y\dot{\lambda} \quad \text{if } \|\mathbf{s}_a\| = \sqrt{2}\tau_y, \tag{71}$$

which, since $G > 0$, $\tau_y > 0$ and $\tau_y' + k' + G > 0$, gives

$$\text{if } \|\mathbf{s}_a\| = \sqrt{2}\tau_y \quad \text{then } \{\mathbf{s}_a \cdot \dot{\mathbf{e}} > 0 \Longleftrightarrow \dot{\lambda} > 0\}. \tag{72}$$

Thus,

$$\{\|\mathbf{s}_a\| = \sqrt{2}\tau_y \text{ and } \mathbf{s}_a \cdot \dot{\mathbf{e}} > 0\} \Rightarrow \dot{\lambda} > 0. \tag{73}$$

On the other hand, if $\dot{\lambda} > 0$, Eq. (67) assures $\|\mathbf{s}_a\| = \sqrt{2}\tau_y$, which together with Eq. (72) asserts that

$$\dot{\lambda} > 0 \Rightarrow \{\|\mathbf{s}_a\| = \sqrt{2}\tau_y \text{ and } \mathbf{s}_a \cdot \dot{\mathbf{e}} > 0\}. \tag{74}$$

Therefore, from Eqs. (73) and (74) we conclude that the yield condition $\|\mathbf{s}_a\| = \sqrt{2}\tau_y$ and the straining condition $\mathbf{s}_a \cdot \dot{\mathbf{e}} > 0$ are sufficient and necessary for plastic irreversibility $\dot{\lambda} > 0$. Considering this and the inequality (66), we thus reveal the following criteria of plastic irreversibility:

$$\dot{\lambda} = \begin{cases} \frac{G\mathbf{s}_a \cdot \dot{\mathbf{e}}}{(\tau_y' + k' + G)\tau_y} > 0 & \text{if } \|\mathbf{s}_a\| = \sqrt{2}\tau_y \quad \text{and} \quad \mathbf{s}_a \cdot \dot{\mathbf{e}} > 0, \\ 0 & \text{if } \|\mathbf{s}_a\| < \sqrt{2}\tau_y \quad \text{or} \quad \mathbf{s}_a \cdot \dot{\mathbf{e}} \leqslant 0. \end{cases} \tag{75}$$

In the ON phase of the switch, $\dot{\lambda} > 0$, the mechanism of plastic irreversibility is working and the material exhibits elastoplastic behavior, while in the OFF phase of the switch, $\dot{\lambda} = 0$, the material behavior is reversible and elastic. According to the complementary trios (65)–(67), there are just two phases: (i) $\dot{\lambda} > 0$ and $\|\mathbf{s}_a\| = \sqrt{2}\tau_y$, and (ii) $\dot{\lambda} = 0$ and $\|\mathbf{s}_a\| \leqslant \sqrt{2}\tau_y$. From the switch (75) it is clear that (i) corresponds to the plastic phase (or the on phase or the elastoplastic phase) while (ii) to the elastic phase (or the off phase).

5.2. Constant strain rate

Now we consider a rectilinear strain path with

$$\dot{\mathbf{e}} = \mathbf{c}, \tag{76}$$

where $\mathbf{c}$ is a given second-order constant deviatoric tensor.

Theorem 6. *For the model* (60)–(67) *subjected to the strain path* (76), *the switch-on time is given by*

$$t_{on} = t_{off} + \frac{\sqrt{B^2 - 4AC} - B}{2A}, \tag{77}$$

where

$$A := 4G^2\|\mathbf{c}\|^2, \quad B := 4G\mathbf{s}_a(t_{off}) \cdot \mathbf{c}, \quad C := \|\mathbf{s}_a(t_{off})\|^2 - 2\tau_y^2(\lambda_{off}) \tag{78}$$

and λ_{off} *denotes the value of* λ *at the latest unloading time* t_{off}. *Then, from the time moment* t_{on} *on we have*

$$\dot{\lambda}(t) > 0 \quad \forall\ t > t_{on}. \tag{79}$$

Proof. For the given strain path (76) and the admissible initial active stress $\mathbf{s}_a(t_{off})$ specified at time $t = t_{off}$, we first integrate Eq. (70) with $\dot{\lambda} = 0$ from t_{off} to t, giving

$$\mathbf{s}_a(t) = \mathbf{s}_a(t_{off}) + 2G(t - t_{off})\mathbf{c}. \tag{80}$$

Then, substituting it into the yield condition $\|\mathbf{s}_a(t)\|^2 = 2\tau_y^2(\lambda_{off})$ generates the following equation for t:

$$A(t - t_{off})^2 + B(t - t_{off}) + C = 0. \tag{81}$$

Because of $A > 0$ and $C \leqslant 0$, we get $B^2 - 4AC \geqslant 0$ and hence $t \geqslant t_{off}$. Taking the inner product of Eq. (80) with $4G(t - t_{off})\mathbf{c}$ gives

$$\begin{aligned} 4G(t - t_{off})\mathbf{s}_a(t) \cdot \mathbf{c} &= 4G\mathbf{s}_a(t_{off}) \cdot \mathbf{c}(t - t_{off}) + 8G^2\|\mathbf{c}\|^2(t - t_{off})^2 = B(t - t_{off}) + 2A(t - t_{off})^2 \\ &= A(t - t_{off})^2 - C, \end{aligned}$$

where Eqs. (78) and (81) were used. We consider only the case of $t > t_{off}$, which together with $A > 0$ and $C \leqslant 0$ leads to

$$\mathbf{s}_a(t) \cdot \mathbf{c} > 0. \tag{82}$$

From Eqs. (81) and (82) and the switch-on criterion (75) we thus conclude that the switch-on time t_{on} is given by Eq. (77), and $\dot{\lambda}(t) > 0$ at this time moment $t = t_{on}$.

In terms of the integrating factor

$$Y(\lambda) := \exp\left[\int_0^{\lambda} \frac{k'(\lambda_1) + G(\lambda_1)}{\tau_y(\lambda_1)}\, d\lambda_1\right], \tag{83}$$

the integral of Eq. (70) can be obtained as follows:

$$\mathbf{s}_{\mathrm{a}}(t)=\frac{1}{Y(\lambda(t))}\left[Y(\lambda(t_i))\mathbf{s}_{\mathrm{a}}(t_i)+\int_{t_i}^{t}2GY(\lambda(\xi))\dot{\mathbf{e}}(\xi)\,\mathrm{d}\xi\right]. \tag{84}$$

Substitution of the above equation for $\mathbf{s}_{\mathrm{a}}$ into Eq. (71) and rearrangement yield

$$\dot{Z}(t)=Y(\lambda(t_i))\mathbf{s}_{\mathrm{a}}(t_i)\cdot\dot{\mathbf{e}}(t)+\int_{t_i}^{t}2GY(\lambda(\xi))\dot{\mathbf{e}}(t)\cdot\dot{\mathbf{e}}(\xi)\,\mathrm{d}\xi, \tag{85}$$

where

$$Z(\lambda):=\int_0^{\lambda}\frac{\tau_{\mathrm{y}}(\lambda_1)Y(\lambda_1)[\tau_{\mathrm{y}}'(\lambda_1)+k'(\lambda_1)+G]}{G}\,\mathrm{d}\lambda_1 \tag{86}$$

is a newly defined irreversibility parameter. Under the strain path (76), from Eq. (85) with its t_i replaced by t_{on} we have

$$\dot{Z}(t)=Y(\lambda(t_{\mathrm{on}}))\mathbf{s}_{\mathrm{a}}(t_{\mathrm{on}})\cdot\mathbf{c}+2G\|\mathbf{c}\|^2\int_{t_{\mathrm{on}}}^{t}Y(\lambda(\xi))\,\mathrm{d}\xi. \tag{87}$$

Since $Y>0$ from Eq. (83) and $\mathbf{s}_{\mathrm{a}}(t_{\mathrm{on}})\cdot\mathbf{c}>0$ as just proved in Eq. (82), the inequality $\dot{Z}(t)\ \forall\ t>t_{\mathrm{on}}$ is verified. The inequality $\dot{\lambda}(t)>0\ \forall\ t>t_{\mathrm{on}}$ follows directly by Eqs. (86) and (69). □

The switching criteria in Eq. (75) and the inequality (79) indicate that for a rectilinear strain path once yielding occurs the model switches-on to the plastic phase and responds always plastically in the subsequent time up to the termination of the strain path.

Before employing the same idea to modify the above conventional mixed-hardening model, we use the group-preserving scheme developed by Liu (2003) to calculate the model responses under a piecewise proportional two-dimensional strain path as shown in Fig. 7(a). The material is linear hardening having $\tau_{\mathrm{y}}=\tau_{\mathrm{y}0}+\tau_{\mathrm{y}}'\lambda$ with $\tau_{\mathrm{y}0}=200$ MPa and $\tau_{\mathrm{y}}'=100$ MPa, and also with $G=20\,000$ MPa and $k'=500$ MPa. Fig. 7 illustrates the response to an input of a cyclic two-triangular path in two dimensions strain space $(\varepsilon_{11},\varepsilon_{12})$, the first cycle of which consists of six pieces from point 0 to point 6. The consecutive cycle repeats in the strain space the locus of the first cycle. The results shown with dashed lines include the stress path in Fig. 7(b), and hysteresis loops in Fig. 7(c) and (d). The response graph of the stress path in Fig. 7(b) as can be seen is very different from the input strain path in Fig. 7(a). One main feature is that the strain path is closed, but the corresponding stress response has an open path. The other feature is that the strain path is composed of straight lines, but the corresponding stress response has straight-line paths in the off phase but destorted arc paths in the on phase due to plasticity and the accompanied hardening effect. As shown in Fig. 7(c) and (d) the original model gives non-smooth stress–strain curves.

5.3. A new model modified from the multi-dimensional mixed-hardening model

In order to overcome the above shortcoming of non-smoothness of the stress–strain curves and adapt the mixed-hardening model to a new one which can simulate cyclic behavior we propose, instead of the continuous shear yield strength function τ_{y}, a modified piecewise-constant shear yield strength given as follows:

$$2(\tau_{\mathrm{y}}^{m})^2:=\|\mathbf{s}_{\mathrm{a}}(t_{\mathrm{off}})\|^2-\frac{\rho^2B^2-[(\rho-1)B+\sqrt{B^2-4AC}]^2}{4\rho^2A}, \tag{88}$$

where A, B and C were defined in Eq. (78). The above t_{off} is the latest unloading (switching-off) time; we may let $t_{\mathrm{off}}=0$ initially. When $\rho=1$, $\tau_{\mathrm{y}}^{m}=\tau_{\mathrm{y}}(\lambda_{\mathrm{off}})$, and we recover to the original non-smooth model. Hereafter we call the model with the above modification the *new model*, and which without considering the above modification the *original model*. Now we prove the following important result.

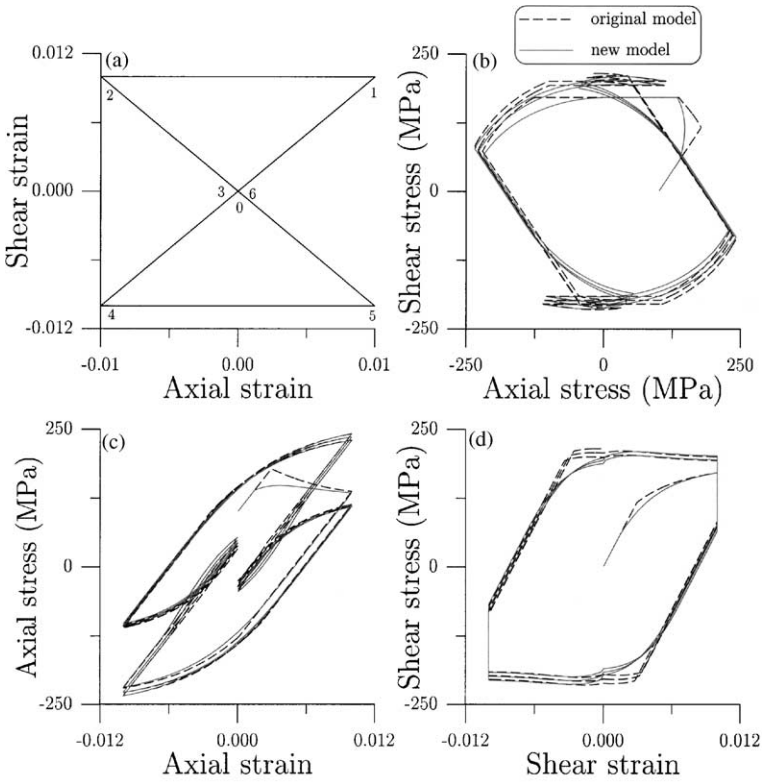

Fig. 7. The responses to an input of a cyclic two-triangular strain path in (a), and displaying the results, respectively, for the original model and for new model in (b) the corresponding stress paths, in (c) the cyclic axial stress–axial strain curves and in (d) the cyclic shear stress–shear strain curves.

Theorem 7. *If* $1 < \rho \leqslant 2$, *then under the strain path* (76) *the switch-on time of the new model is given by*

$$t_{\text{on}} = t_{\text{off}} + \frac{\sqrt{B^2 - 4AC} - B}{2\rho A} \tag{89}$$

and then

$$\dot{\lambda}(t) > 0 \quad \forall\, t > t_{\text{on}}. \tag{90}$$

Proof. For the strain path given by Eq. (76) and the admissible initial active stress $\mathbf{s}_{\text{a}}(t_{\text{off}})$ specified at time $t = t_{\text{off}}$, [4] substituting the elastic constitutive equation (80) into the new yield condition $\|\mathbf{s}_{\text{a}}(t)\|^2 = 2(\tau_{\text{y}}^m)^2$ generates the following equation for t:

$$A(t - t_{\text{off}})^2 + B(t - t_{\text{off}}) + \|\mathbf{s}_{\text{a}}(t_{\text{off}})\|^2 - 2(\tau_{\text{y}}^m)^2 = 0. \tag{91}$$

[4] The admissible stress for the new model is $\|\mathbf{s}_{\text{a}}\| < \sqrt{2}\tau_{\text{y}}$. If $\|\mathbf{s}_{\text{a}}\| = \sqrt{2}\tau_{\text{y}}$ at a time moment then under the loading condition the active stress point will always lie on the yield surface. Mathematically speaking, the yield surface is an invariant surface for the new model, and sometimes we call it a limiting surface because it is an attracting surface of all active stress orbits under proportional loading conditions.

The inner product of Eq. (80) with $4G(t-t_{\text{off}})\mathbf{c}$ gives

$$4G(t-t_{\text{off}})\mathbf{s}_{\text{a}}(t)\cdot\mathbf{c}=4G\mathbf{s}_{\text{a}}(t_{\text{off}})\cdot\mathbf{c}(t-t_{\text{off}})+8G^2\|\mathbf{c}\|^2(t-t_{\text{off}})^2=B(t-t_{\text{off}})+2A(t-t_{\text{off}})^2$$
$$=A(t-t_{\text{off}})^2-\frac{\rho^2B^2-[(\rho-1)B+\sqrt{B^2-4AC}]^2}{4\rho^2A}, \tag{92}$$

where Eqs. (91), (78) and (88) were used. Solving Eq. (91) for t and using Eq. (88) again we obtain

$$t=t_{\text{off}}+\frac{\sqrt{B^2-4AC}-B}{2\rho A}. \tag{93}$$

Substituting it into the right-hand side of Eq. (92) gives

$$4G(t-t_{\text{off}})\mathbf{s}_{\text{a}}(t)\cdot\mathbf{c}=\frac{[(\rho-1)B+\sqrt{B^2-4AC}]^2+[\sqrt{B^2-4AC}-B]^2-\rho^2B^2}{4\rho^2A}. \tag{94}$$

To proceed we consider two cases: $\rho=2$ and $1<\rho<2$. If $\rho=2$, Eq. (94) reduces to

$$8G(t-t_{\text{off}})\mathbf{s}_{\text{a}}(t)\cdot\mathbf{c}=-C. \tag{95}$$

It is obvious that $t=t_{\text{off}}$ implies $C=0$. So we consider the case of $t>t_{\text{off}}$ and $C<0$, and hence

$$\mathbf{s}_{\text{a}}(t)\cdot\mathbf{c}>0. \tag{96}$$

The above inequality together with Eq. (93) asserts that such t is a switch-on time, and thus Eq. (89) holds.

For the case $1<\rho<2$, in order to prove the above inequality (96) we need further to consider two possible conditions, namely $B\geqslant 0$ and $B<0$. From Eq. (94) it follows that

$$4G(t-t_{\text{off}})\mathbf{s}_{\text{a}}(t)\cdot\mathbf{c}=\frac{[\sqrt{B^2-4AC}+(\rho-1)B][\sqrt{B^2-4AC}-B]}{2\rho^2A}. \tag{97}$$

Under the condition $B\geqslant 0$, Eq. (96) follows directly because of $\rho>1$, $A>0$, $C<0$, and hence $\sqrt{B^2-4AC}-B>0$. Now, we turn to the condition $B<0$ which, due to $1<\rho<2$, leads to

$$\sqrt{B^2-4AC}+(\rho-1)B>\sqrt{B^2-4AC}+B$$

and hence

$$4G(t-t_{\text{off}})\mathbf{s}_{\text{a}}(t)\cdot\mathbf{c}>\frac{-2C}{\rho^2} \tag{98}$$

by Eq. (97). So, under the conditions of $t>t_{\text{off}}$ and $C<0$, Eq. (96) follows directly. From Eqs. (93) and (96) we thus conclude that the switch-on time t_{on} of the new model is given by Eq. (89). The proof of inequality (90) is the same as that given in the proof of Theorem 6. □

The above results show that for a rectilinear strain path once yielding occurs the new model responds always in the plastic phase up to the termination of the input. The specification of τ_{y}^m to be the new shear yield strength is equivalent to shorten the original switching-on time given by Eq. (77) to that given by Eq. (89) with a factor $\rho>1$. The smoothing factor ρ cannot be larger than two because it may violate the inequality (90) under some initial conditions. Furthermore, we can prove the following result.

Theorem 8. *The modified shear yield strength τ_{y}^m in the new model satisfies the following inequality*

$$\tau_{\text{y}}^m<\tau_{\text{y}}(\lambda_{\text{off}}). \tag{99}$$

Proof. Upon letting $t = t_{on}$ in Eqs. (81) and (91), and noting that the $t_{on} - t_{off}$ in the second equation is the $t_{on} - t_{off}$ in the first equation dividing by ρ when comparing Eq. (77) with Eq. (89), we obtain

$$A(t_{on} - t_{off})^2 + B(t_{on} - t_{off}) + \|\mathbf{s}_a(t_{off})\|^2 - 2\tau_y^2(\lambda_{off}) = 0, \tag{100}$$

$$\frac{A}{\rho^2}(t_{on} - t_{off})^2 + \frac{B}{\rho}(t_{on} - t_{off}) + \|\mathbf{s}_a(t_{off})\|^2 - 2(\tau_y^m)^2 = 0. \tag{101}$$

From Eqs. (65) and (100) it follows that

$$A(t_{on} - t_{off})^2 + B(t_{on} - t_{off}) \geqslant 0. \tag{102}$$

Then, subtracting Eq. (101) from Eq. (100) we get

$$2\tau_y^2(\lambda_{off}) - 2(\tau_y^m)^2 = A(t_{on} - t_{off})^2\left(1 - \frac{1}{\rho^2}\right) + B(t_{on} - t_{off})\left(1 - \frac{1}{\rho}\right). \tag{103}$$

Because of $\rho > 1$ and $A > 0$, from the above equation it follows that

$$2\tau_y^2(\lambda_{off}) - 2(\tau_y^m)^2 > \left(1 - \frac{1}{\rho}\right)[A(t_{on} - t_{off})^2 + B(t_{on} - t_{off})]. \tag{104}$$

Due to $\rho > 1$ and Eq. (102) we prove inequality (99). □

5.4. Characterization of new model behavior

The method employed in the new model amounts to modify the $\dot{\lambda}$ in Eq. (70) by subjecting to the new switching criteria:

$$\dot{\lambda} = \frac{G\mathbf{s}_a \cdot \dot{\mathbf{e}}}{(\tau_y' + k' + G)\tau_y} > 0 \quad \text{if } \sqrt{2}\tau_y(\lambda_{off}) > \|\mathbf{s}_a\| \geqslant \sqrt{2}\tau_y^m \quad \text{and} \quad \mathbf{s}_a \cdot \dot{\mathbf{e}} > 0, \tag{105}$$

$$\dot{\lambda} = 0 \quad \text{if } \|\mathbf{s}_a\| < \sqrt{2}\tau_y^m \quad \text{or} \quad \mathbf{s}_a \cdot \dot{\mathbf{e}} \leqslant 0. \tag{106}$$

In the ON phase of the switch, $\dot{\lambda} > 0$, the mechanism of plastic irreversibility is working and the material modeled by the new model exhibits elastoplastic behavior, while in the OFF phase of the switch, $\dot{\lambda} = 0$, the material behavior is reversible and elastic. We note again that as the original model is, the new model is thermodynamically consistent since $\dot{\lambda} > 0$ in the plastic phase and $\dot{\lambda} = 0$ in the elastic phase.

Inserting the two $\dot{\lambda}$'s in Eqs. (105) and (106) into Eq. (70) the governing equations for active stress of the new model are found to be

$$\dot{\mathbf{s}}_a = 2G\dot{\mathbf{e}} - \frac{G(k' + G)\mathbf{s}_a \cdot \dot{\mathbf{e}}}{\tau_y^2(\tau_y' + k' + G)}\mathbf{s}_a \quad \text{if } \sqrt{2}\tau_y(\lambda_{off}) > \|\mathbf{s}_a\| \geqslant \sqrt{2}\tau_y^m \text{ and } \mathbf{s}_a \cdot \dot{\mathbf{e}} > 0, \tag{107}$$

$$\dot{\mathbf{s}}_a = 2G\dot{\mathbf{e}} \quad \text{if } \|\mathbf{s}_a\| < \sqrt{2}\tau_y^m \text{ or } \mathbf{s}_a \cdot \dot{\mathbf{e}} \leqslant 0. \tag{108}$$

In the new model we really depress the original shear yield stress level τ_y to a lower level τ_y^m, and when $\|\mathbf{s}_a\| = \sqrt{2}\tau_y^m$ we call the material yielding. [5] It allows plasticity occurring in a finite stress volume in $\sqrt{2}\tau_y > \|\mathbf{s}_a\| \geqslant \sqrt{2}\tau_y^m$ as schematically shown in Fig. 8. Mathematically speaking, e.g. Hale (1969), a set $\mathscr{F}$

[5] The yielding defined here is different from that for the original model. For distinct we may call it subyielding as that suggested by Hashiguchi (1989).

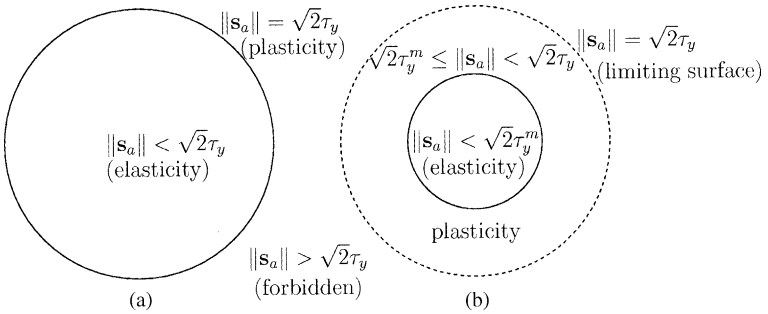

Fig. 8. Allowable active stress regions for (a) original mixed-hardening elastoplastic model and (b) newly modified mixed-hardening elastoplastic model.

in $\mathbb{R}^{3\times3}\otimes\mathbb{R}$ is said to be an *invariant set* of Eqs. (107) and (105) if, for any point $\mathbf{p}\in\mathscr{F}$ the solution curve through $\mathbf{p}$ belongs to $\mathscr{F}$ for t in $(-\infty,\infty)$. Let us define the set by $\mathscr{F}:=\{(\mathbf{s}_a,\lambda)|\|\mathbf{s}_a\|-\sqrt{2}\tau_y(\lambda)=0\}$. Taking the time derivative of $\|\mathbf{s}_a\|-\sqrt{2}\tau_y(\lambda)$ and feeding Eq. (107) for $\dot{\mathbf{s}}_a$ and Eq. (105) for $\dot{\lambda}$ it is obvious that $\dot{\mathscr{F}}=0$. It means that the original yield surface $\|\mathbf{s}_a\|-\sqrt{2}\tau_y=0$ is an invariant surface for the new model. However, we sometimes call it a *limiting surface* because it is an attracting set of all orbits of $(\mathbf{s}_a,\lambda)$ under proportional loading conditions. [6]

Because the original model and the new model share the same governing equation (70) and the same $\dot{\lambda}$, Eq. (87) with its t_{on}'s replaced by the new t_{on} defined in Eq. (89) is still applicable to the new model when it subjects to the strain path (76). Especially, for the new model the active stress formula is also given by Eq. (84); however, the initial active stress $\mathbf{s}_a(t_{on})$ does not necessarily locate on the yield surface. Indeed, for the new model we only allow $\|\mathbf{s}_a(t_{on})\|=\sqrt{2}\tau_y^m<\sqrt{2}\tau_y(\lambda_{off})$.

In cyclic plasticity theory, various phenomena of material behavior have been characterized in order to facilitate our description of stress–strain curves under different loading conditions. A theoretical model is performing well if it is able to reproduce all these phenomena of cyclic plasticity. According to the new models we have demonstrated some observed phenomena and effects through one-dimensional illustrative calculation examples. Now we calculate the responses of the above modified multi-dimensional mixed-hardening model under the input given in Fig. 7(a) again. The smoothing factor used in this calculation is $\rho=2$. The results shown with solid lines include the stress path in Fig. 7(b), and hysteresis loops in Fig. 7(c) and (d). As shown the new model gives smooth stress–strain curves.

For the general strain path we need to calculate the switching-on time in order to provide a similar method to smooth the model responses. Substituting the elastic equation

$$\mathbf{s}_a(t)=\mathbf{s}_a(t_{off})+2G[\mathbf{e}(t)-\mathbf{e}(t_{off})] \tag{109}$$

into the yield condition $\|\mathbf{s}_a(t)\|^2=2\tau_y^2(\lambda_{off})$ generates usually a nonlinear equation for t as follows:

$$\|\mathbf{s}_a(t_{off})\|^2+4G\mathbf{s}_a(t_{off})\cdot[\mathbf{e}(t)-\mathbf{e}(t_{off})]+4G^2\|\mathbf{e}(t)-\mathbf{e}(t_{off})\|^2-2\tau_y^2(\lambda_{off})=0. \tag{110}$$

[6] The limiting surface was understood here from a mathematical sense as just explored. However, in plural surfaces theory of unconventional type they may be bestowed some different or same names, such as bounding surface (Dafalias and Popov, 1975), limiting surface (Krieg, 1975), normal-yield surface (Hashiguchi, 1989), etc. Moreover, they may be setting from a geometric sense rather than from a mathematical sense.

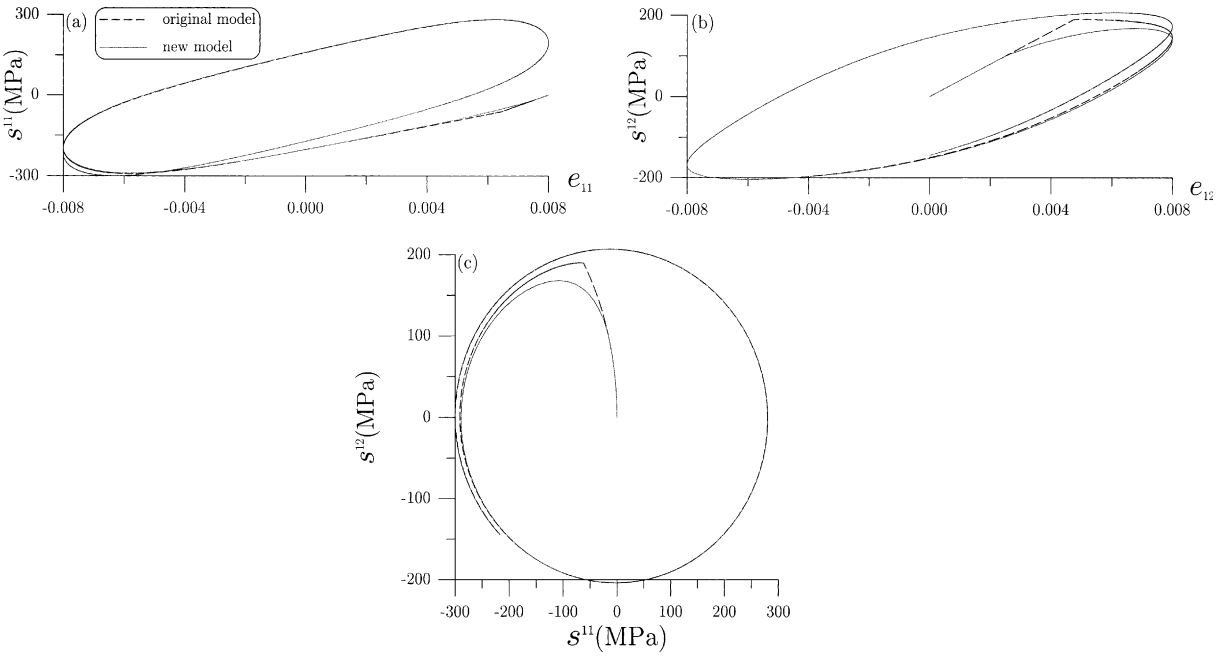

Fig. 9. The responses to a non-proportional circular strain path are displaying, respectively, for the original model and for new model in (a) the cyclic axial stress–axial strain curves, in (b) the cyclic shear stress–shear strain curves and in (c) the corresponding stress paths.

Solve this equation numerically and denote the solution by t_{on}^{o}. Then, we replace it by a new switching-on time

$$t_{\text{on}} = t_{\text{off}} + \frac{t_{\text{on}}^{\text{o}} - t_{\text{off}}}{\rho}. \tag{111}$$

After this time the new model is in the plastic phase, and the numerical scheme [7] is used to calculate the response until an unloading occurs. The modified shear yield stress can be obtained by inserting the t_{on} in Eq. (111) into Eq. (110) to replace their t's and replacing $\tau_{\text{y}}^2(\lambda_{\text{off}})$ by $(\tau_{\text{y}}^m)^2$, i.e.,

$$2(\tau_{\text{y}}^m)^2 = \|\mathbf{s}_{\text{a}}(t_{\text{off}})\|^2 + 4G\mathbf{s}_{\text{a}}(t_{\text{off}}) \cdot [\mathbf{e}(t_{\text{on}}) - \mathbf{e}(t_{\text{off}})] + 4G^2\|\mathbf{e}(t_{\text{on}}) - \mathbf{e}(t_{\text{off}})\|^2. \tag{112}$$

This equation is however an implicit form for τ_{y}^m, and not likes the one in Eq. (88) for rectilinear strain path. We should note that the modified shear yield stress is path dependent.

Below we give a numerical example for the new model under a non-proportional two-dimensional strain path given by $e_{11} = e_0 \cos(2\pi t/100)$ and $e_{12} = e_{21} = e_0 \sin(2\pi t/100)$ with $e_0 = 0.008$, and the other components being zero. The corresponding hysteretical loops and stress path are shown in Fig. 9 (a), (b) and (c), respectively. It can be seen that the new model gives a quite smooth stress path than that given by the original model.

[7] Because for the new model stress points are not confined on the yield surface, any effective numerical scheme for ODEs, e.g. the Runge–Kutta method, can be used to calculate the responses through integrating Eqs. (105) and (107) in the plastic phase. However, for the original model we have to require the numerical scheme to match the consistency condition, e.g. the radial return method, such that the stress points are guaranteed to locate on the yield surface.

6. Conclusions

In this paper we have proposed simple but critical modifications of the one-dimensional perfectly elastoplastic model, of the one-dimensional bilinear elastoplastic model as well as of the one-dimensional mixed-hardening elastoplastic model, by merely including a smooth factor ρ, which is proved to be $1 < \rho \leqslant 2$. When $\rho = 1$ the original models are recovered. The main idea is to replace the yield surface by a new concept of yield volume through the specification of a piecewise constant yield stress. Hence, plasticity is allowed to happen in a non zero-measure domain in stress space. In doing so, we have a degree of freedom to adjust the smoothness of stress–strain curve. Numerical tests were conducted by subjecting the modified models to monotonic loadings and cyclic loadings. The major phenomenological cyclic behavior of metals can be simulated, which include strain hardening, cyclic hardening, the Bauschinger effect, as well as strain ratcheting. Comparing the stress–strain curves obtained from the original model and from the new model confirms that the proposed modification not only makes a significant improvement of the qualitative behavior but also increases the model simulation capability. Finally, we extended the modification to the multi-dimensional mixed-hardening elastoplastic model, and demonstrated that the original yield surface has to be viewed mathematically as a limiting surface of the new model. For computing the new model has the advantage that it need not to match the consistency condition and is more easily to numerically implement than the original model, since stress points are not confined on the yield surface, and hence the conventional numerical design to match the consistency condition is now no more needed.

Acknowledgement

The financial support provided by the National Science Council under Grant NSC 91-2212-E-019-003 is gratefully acknowledged.

References

Armstrong, P.J., Frederick, C.O., 1966. A mathematical representation of the multiaxial Bauschinger effect. G.E.G.B. Report RD/B/N 731.

Auricchio, F., Beirão da Veiga, L., 2003. On a new integration scheme for von-Mises plasticity with linear hardening. Int. J. Numer. Meth. Engng. 56, 1375–1396.

Auricchio, F., Taylor, R.L., 1995. Two material models for cyclic plasticity: nonlinear kinematic hardening and generalized plasticity. Int. J. Plast. 11, 65–98.

Besseling, J.F., 1958. A theory of elastic, plastic and creep deformations of an initially isotropic material showing anisotropic strain hardening, creep recovery and secondary creep. J. Appl. Mech. ASME 25, 529–536.

Caddemi, S., 1994. Computational aspects of the integration of the von Mises linear hardening constitutive laws. Int. J. Plast. 10, 935–956.

Chaboche, J.L., 1986. Time-independent constitutive theories for cyclic plasticity. Int. J. Plast. 2, 149–188.

Chaboche, J.L., 1991. On some modifications of kinematic hardening to improve the description of ratcheting effects. Int. J. Plast. 7, 661–678.

Chaboche, J.L., Rousselier, G., 1983. On the plastic and viscoplastic constitutive equations. J. Press. Vess. Technol. ASME 105, 153–164.

Chiang, D.Y., 1999. The generalized Masing models for deteriorating hysteresis and cyclic plasticity. Appl. Math. Modell. 23, 847–863.

Dafalias, Y.F., 1984. Modelling cyclic plasticity: simplicity versus sophistication. In: Desai, C.S., Gallagher, R.H. (Eds.), Mechanics of Engineering Materials. John Wiley and Sons, New York, pp. 153–178.

Dafalias, Y.F., Popov, E.P., 1975. A model of nonlinearly hardening materials for complex loading. Acta Mech. 21, 173–192.

Dafalias, Y.F., Popov, E.P., 1976. Plastic internal variables formalism of cyclic plasticity. J. Appl. Mech. ASME 98, 645–651.

Drucker, D.C., 1988. Conventional and unconventional plastic response and representation. Appl. Mech. Rev. ASME 41, 151–167.

Drucker, D.C., Palgen, L., 1981. On stress–strain relations suitable for cyclic and other loadings. J. Appl. Mech. ASME 23, 479–485.

Hale, J.K., 1969. Ordinary Differential Equations. Wiley, New York.
Hashiguchi, K., 1988. A mathematical modification of two surface model formulation in plasticity. Int. J. Solids Struct. 24, 987–1001.
Hashiguchi, K., 1989. Subloading surface model in unconventional plasticity. Int. J. Solids Struct. 25, 917–945.
Hashiguchi, K., 1993. Mechanical requirements and structures of cyclic plasticity models. Int. J. Plast. 9, 721–748.
Hodge Jr., P.G., 1957. Discussion of Prager (1956). J. Appl. Mech. ASME 23, 482–484.
Hong, H.-K., Liu, C.-S., 1993. Reconstructing J_2 flow model for elastoplastic materials. Bull. College Engng. N.T.U. 57, 95–114.
Hong, H.-K., Liu, C.-S., 1997. Prandtl–Reuss elastoplasticity: on–off switch and superposition formulae. Int. J. Solids Struct. 34, 4281–4304.
Hong, H.-K., Liu, C.-S., 1999. Internal symmetry in bilinear elastoplasticity. Int. J. Non-Linear Mech. 34, 279–288.
Iwan, W.D., 1966. A distributed element model for hysteresis and its steady-state dynamic response. J. Appl. Mech. ASME 33, 893–900.
Iwan, W.D., 1967. On a class of models for the yielding behavior of continuous and composite systems. J. Appl. Mech. ASME 34, 612–617.
Krieg, R.D., 1975. A practical two surface plasticity theory. J. Appl. Mech. ASME 42, 641–646.
Liu, C.-S., 1997. Exact solutions and dynamic responses of SDOF bilinear elastoplastic structures. J. Chin. Inst. Engrs. 20, 511–525.
Liu, C.-S., 2000. The steady loops of SDOF perfectly elastoplastic structures under sinusoidal loadings. J. Marine Sci. Tech. 8, 50–60.
Liu, C.-S., 2001. Cone of non-linear dynamical system and group preserving schemes. Int. J. Non-Linear Mech. 36, 1047–1068.
Liu, C.-S., 2002. The steady-state responses of a bilinear elastoplastic oscillator under sinusoidal loading. J. Chin. Inst. Engrs. 25, 199–210.
Liu, C.-S., 2003. A consistent numerical scheme for the von Mises mixed-hardening constitutive equations. Int. J. Plast., in press.
Mróz, Z., 1967. On the description of anisotropic workhardening. J. Mech. Phys. Solids 15, 163–175.
Mróz, Z., 1969. An attempt to describe the behavior of metals under cyclic loads using a more general work-hardening model. Acta Mech. 7, 199–215.
Mróz, Z., Norris, V.A., Zienkiewicz, O.C., 1979. Application of an anisotropic hardening model in the analysis of elasto-plastic deformation of soils. Geotechnique 29, 1–34.
Mróz, Z., Norris, V.A., Zienkiewicz, O.C., 1981. An anisotropic, critical state model for soils subjected to cyclic loading. Geotechnique 31, 451–469.
Ohno, N., 1990. Recent topics in constitutive modeling of cyclic plasticity and viscoplasticity. Appl. Mech. Rev. ASME 43, 283–295.
Prager, W., 1956. A new method of analyzing stresses and strains in work-hardening plastic solids. J. Appl. Mech. ASME 23, 493–496.
Wen, Y.K., 1976. Method for random vibration of hysteretic systems. J. Engng. Mech. ASCE 102, 249–263.
Ziegler, H., 1959. A modification of Prager's hardening rule. Quat. J. Appl. Math. 17, 55–65.